Journal of Engineering Mathematics **50:** 343–358, 2004.

Impact of two circular plates one of which is floating on a thin layer of liquid

A.A. KOROBKIN and M. OHKUSU[1]
Lavrentyev Institute of Hydrodynamics, Novosibirsk 630090, Russia; [1]*RIAM, Kuyshu University, Fukuoka; Japan*

Received 5 March 2002; accepted in revised form 28 June 2004

Abstract. The paper deals with the axisymmetric unsteady problem of the collision of two circular plates, one of which is located initially on the surface of a shallow liquid layer and another is falling down on it. The presence of air between the colliding plates is taken into account. Both the air and the liquid are assumed ideal and incompressible and their flows potential. The flows in the liquid layer and between the p1ates are assumed one-dimensional with corrections for three-dimensional effects close to the plate edges. The present study is focused on the stage of strong interaction between the plates, during which the floating plate is accelerated and the hydrodynamic pressure in the liquid layer takes its maximum value. A simplified model of this interaction is suggested. Velocities of the plates and the hydrodynamic pressure on the bottom of the liquid layer are analytically estimated and compared with experimental results. The model provides the maximum of the hydrodynamic pressure, which can be used at the design stage. It is shown that the air flow between the moving plates is of major importance to explain the low amplitude of the measured hydrodynamic pressures.

Key words: air-cushion, effect, circular plates, hydrodynamic loads, thin liquid layer, water impact

1. Introduction

The axisymmetric unsteady problem of the collision of two circular plates, one of which is placed initially on the boundary of a liquid layer, is considered. This study was motivated by experiments performed by Ermanyuk [1] with two colliding plates (experimental setup is shown in Figure 1). An analysis of the experimenta1 results is given by Ermanyuk and Ohkusu [2]. The authors of the present paper participated in the design of these experiments. An original purpose of the experiments was to measure acoustic pressures in a shallow liquid layer caused by the impact onto a floating plate. The hydrodynamic pressures were expected to be much higher than the 'water hammer' pressure $\rho V_n c_0$, where ρ is the liquid density, V_n is the normal velocity of the body surface at the impact instant and c_0 is the sound speed in the liquid at rest, owing to multiple reflections of the shock wave generated by the impact from both the bottom and the disk. For a circular disk, the radius of which R is much greater than the liquid depth h, it was expected that the maximum of the hydrodynamic pressure occurs at the center of the disk at the time instant, when the relief waves originated at the periphery of the floating disk come to its center. However, the experiments revealed much smaller pressures than expected. Moreover, the measured pressures were smaller than the 'water hammer' pressure, which should be expected for a liquid of infinite depth in the case of an impulsive start of a floating plate. A wavelet analysis of the pressure evolution was performed in [2]. It was concluded that the main time-scale that corresponds to the maximum of the wavelet spectrum is presumably defined by the effect of air flow from the gap between the disks during the collision. The aim of the present paper is to show that the presence of the

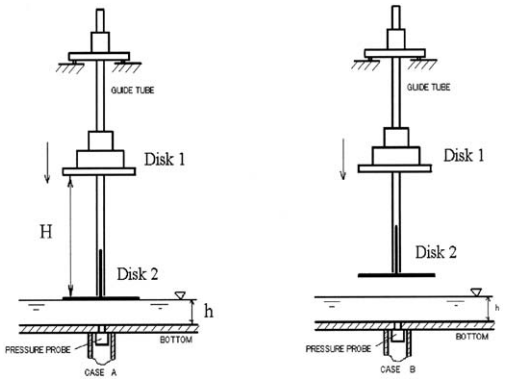

Figure 1. Experimental setup (form Ermanyuk [1]).

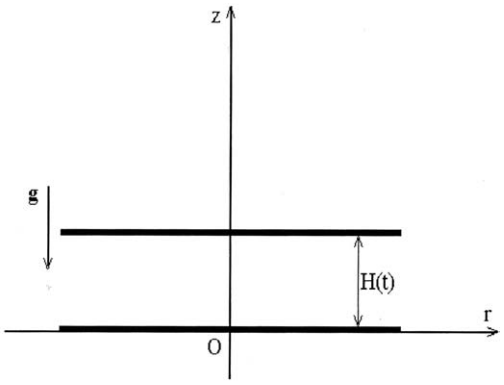

Figure 2. Collision of two circular plate, the upper of which is falling down due to gravity.

air between the colliding disks plays an important role and may control the amplitude of the hydrodynamic loads.

In the problem of floating-body impact it is usually assumed that both the body and the liquid are initially at rest and the body begins suddenly to move at a prescribed velocity. For a liquid of infinite depth the maximum of the hydrodynamic pressure occurs during the initial stage when the liquid compressibility is of major significance [3]. This maximum is known as the 'water hammer' pressure, and is equal to $\rho c_0 V_n$ for impact velocities up to several meters per second. In the case of a body floating on the water surface ($\rho = 1000$ kg m^{-3}, $c_0 = 1500$ m sec^{-1}) and starting suddenly to move down at a velocity of $1{\cdot}7$ m sec^{-1}, we obtain $\rho c_0 V_n = 2{\cdot}6 \times 10^6$ N m^{-2}. The velocity of $1{\cdot}7$ m sec^{-1} is that of a body falling due to the gravity from the height of 15 cm. Such high pressures were not measured in experiments by Ermanyuk [1]. It is usually believed that such high pressures are not detected due to poor resolution provided by commonly used pressure gauges; this is the natural period of pressure ganges used in the experiments may be greater than the duration of the acoustic pressures. However, the experiments by Ermanyuk [1] were specially designed to measure such pressure pulses of short duration. The present study is based on the idea that a flat disk falling down cannot provide an impulsive start of the floating disk. It is shown that the presence of air between the colliding plates leads to a finite acceleration of the floating disk. Even if the acceleration is relatively high, the floating-disk motion still cannot be treated as impulsive and the maximum of the hydrodynamic loads is dependent on the rate of the penetration-velocity increase.

The air cannot escape immediately from the gap between the disks, which makes the process of the body interaction longer and reduces the maximal acceleration of the floating body. The presence of the air may be responsible for a reduction of the hydrodynamic loads on the floating body. This effect can be explained even within the incompressible ideal-fluid model of the air flow. In the case of two colliding plates one of which is at rest and another one falling onto it vertically, this effect was studied qualitatively by Yih [4]. The latter problem is revisited in Section 2, in order to evaluate the evolution in time of both the pressure in the thin air layer between the plates and the thickness of this layer. The problem of two colliding disks, one of which is initially at rest and free to move owing to another disk falling onto it vertically, is analyzed in Section 3. The original problem of two circular plates, one of which

floats initially on the surface of a thin liquid layer, is investigated in Section 4. The investigation is focused on the pressure evolution in the liquid layer. The theoretical predictions are compared to experimental results by Ermanyuk [1] for the pressure on the liquid bottom. The theoretical pressures are slightly higher than the measured ones but the analysis explains well the reduction of the loads due to finite acceleration of the floating plate. The presented model can be used to estimate the maximal hydrodynamic pressures for two colliding bodies with flat surfaces in the impact region. However, the model cannot predict oscillations after the pressure peak, which are well-pronounced in the experimental curves and may be attributed to the acoustic effects (see [2] for details).

2. Approximate model in the case of a fixed lower plate

Two circular plates, the lower of which is fixed and the upper is falling down on it due to gravity, are considered (see Figure 2), The origin of the cylindrical coordinate system Orz is taken at the centre of the lower plate. Initially ($t = 0$) the upper plate is placed at a distance H_0 above the lower one. The plates are of radius R and perfectly rigid. The elasticity of the impacting plates is not taken into account in the present study. The interaction between the plates can be neglected during the acceleration stage of the process, when the distance $H(t)$ between the plates is larger than or comparable with the plate radius R. At this stage the upper plate falls down as if the fluid is unbounded. As a first-order approximation, the velocity $V(t)$ of the moving disk is given by the formula $V(t) = gt$, which does not account for aerodynamic forces. If the presence of air between the plates is not taken into account, the plates collide at the instant $T = \sqrt{2H_0/g}$ with the velocity $V_c = \sqrt{2gH_0}$, where g is the acceleration due to gravity. This is the case of rigid impact.

The presence of the air, which can be approximately neglected during the acceleration stage, is of major significance during the next stage which is referred to as the interaction stage. At the interaction stage the distance $H(t)$ between the plates is much smaller than the plate radius R, $H(t)/R \ll 1$, and the air is forced to flow from the region $D(t) = \{r, z | r < R, 0 < z < H(t)\}$ between the plates. The velocity of the falling plate decays due to its strong interaction with the lower plate and is much smaller than the radial velocity of the air outflow. This implies that the 'thin-layer' approximation can be used to describe both the air flow and the pressure between the plates.

The resistance of the fluid outside $D(t)$ to the flow from between the plates is assumed negligible and is not taken into account below. This means, in particular, that the fluid particles, which left the region $D(t)$ at an instant τ, move thereafter at the velocity $u_r(R, \tau)$, where $u_r(r, t)$ is the radial velocity of the air flow in $D(t)$. These particles form a jet, in which the pressure is equal to the atmospheric pressure. Therefore, the pressure at the plate edge, $r = R$, is also atmospheric at any instant of time within the considered approximation. This assumption highly simplifies the analysis and is based on experiments with a plate falling onto a table [4].

We assume that the air is an ideal and incompressible fluid and that its flow is potential. Both viscous effects and the compressibility of the air may be of importance at the very final stage, when the plates are very close to each other. The significance of both the viscous and the elastic properties of the air in $D(t)$ depends on the falling body mass M, the drop height H_0 and the plate radius R, and can be verified by analyzing the solution obtained within the ideal and incompressible air model.

Within the framework of these assumptions the axisymmetric air flow between the plates during the interaction stage is described by the velocity potential $\phi(r, z, t)$, for which the boundary-value problem has the form

$$\frac{\partial^2\phi}{\partial r^2} + \frac{1}{r}\frac{\partial\phi}{\partial r} + \frac{\partial^2\phi}{\partial z^2} = 0 \quad (0 < z < H(t), 0 < r < R), \tag{1}$$

$$\frac{\partial\phi}{\partial z} = 0 \quad (z = 0, 0 < r < R), \tag{2}$$

$$\frac{\partial\phi}{\partial z} = \frac{\mathrm{d}H}{\mathrm{d}t}(t) \quad (z = H(t), 0 < r < R), \tag{3}$$

$$p(r, z, t) = -\rho_a\left(\frac{\partial\phi}{\partial t} + \frac{1}{2}|\nabla\phi|^2\right), \quad (0 < z < H(t), 0 < r < R), \tag{4}$$

$$p(R, z, t) = 0, \tag{5}$$

where ρ_a is the air density and $p(r, z, t)$ is the deviation of the pressure between the plates from the atmospheric pressure.

The boundary-value problem (1–5) has to be solved together with the equation of the falling plate motion, which follows from Newton's second law

$$M\frac{\mathrm{d}^2H}{\mathrm{d}t^2} = -Mg + F_a(t), \tag{6}$$

where $F_a(t)$ is the aerodynamic force on the moving plate

$$F_a(t) = 2\pi\int_0^R rp(r, H(t), t)\mathrm{d}r. \tag{7}$$

Formally speaking, Equations (1–5) are valid only during the interaction stage, when $H(t)/R \ll 1$. The duration of this stage is unknown in advance and has to be determined together with the solution of the problem. Initial conditions for Equation (6) can be obtained by matching the solution at the interaction stage with that at the acceleration stage. We use another idea assuming that Equations (1–5) are valid during both the interaction and the acceleration stages. If so, the initial conditions for Equation (6) have the form

$$H(0) = H_0, \qquad \frac{\mathrm{d}H}{\mathrm{d}t}(0) = 0. \tag{8}$$

It will be shown that the force $F_a(t)$ in (6) evaluated with the help of Equations (1–5) and (7), is much smaller than the gravity force Mg and Equation (6) can be approximated as $\mathrm{d}^2H/\mathrm{d}t^2 = -g$ during the acceleration stage. This implies that the initial conditions (8) for the 'thin-layer' model (1–7) do not disturb essentially the motion of the falling plate at the acceleration stage, when $H(t) \approx H_0 - gt^2/2$.

Equations (1–3) are satisfied by the following function

$$\phi(r, z, t) = -\frac{\dot{H}}{4H}(r^2 - 2z^2) + \phi_0(t); \tag{9}$$

this can be verified by substitution. A dot stands for the time derivative. The pressure distribution (4) is written as

$$p(r, z, t) = \rho_a\left[r^2\left(\frac{\ddot{H}}{4H} - \frac{3\dot{H}^2}{8H^2}\right) - z^2\frac{\ddot{H}}{2H} - \dot{\phi}_0(t)\right], \tag{10}$$

where $0 < r < R$ and $0 < z < H(t)$. The second term in expression (10) for $r = R$ can be neglected in comparison with the first with a relative error of $O(H^2/R^2)$ during the interaction stage. The boundary condition (5) is satisfied with the same relative error if one takes

$$\dot{\phi}_0(t) = R^2 \left(\frac{\ddot{H}}{4H} - \frac{3\dot{H}^2}{8H^2} \right)$$

We obtain the approximate pressure distribution between the plates

$$p(r, t) \approx \rho_a (R^2 - r^2) \left(\frac{3\dot{H}^2}{8H^2} - \frac{\ddot{H}}{4H} \right), \tag{11}$$

which does not depend on the vertical coordinate z.

Substituting (11) in (7), we find

$$F_a(t) = \frac{\pi}{8} \rho_a R^4 \left(\frac{3\dot{H}^2}{2H^2} - \frac{\ddot{H}}{H} \right). \tag{12}$$

A force of the same magnitude acts also on the lower fixed plate.

Combining Equations (11) and (12), the formula for the pressure can be presented in the form

$$p(r, z, t) = \frac{8F_a(t)}{\pi R^2} \left(1 - \frac{r^2}{R^2} \right). \tag{13}$$

It is seen that the pressure maximum, $p_{\max} = 8F_a(t)/(\pi R^2)$, occurs at the centre of the region, $r = 0$. The radial velocity of the air flow, $u_r = \partial\phi/\partial r$, follows from (9) and is given by

$$u(r, t) = -\frac{\dot{H}}{2H} r \tag{14}$$

with the outflow velocity $u_r(R, t)$ being $-\dot{H}R/(2H)$.

Substituting (12) in the motion equation (6) and introducing the non-dimensional variables $\zeta(\tau) = H(t)/H_0$ and $\tau = t/T$, we arrive at the following problem with respect to the new unknown function $\zeta(\tau)$

$$\left(1 + \frac{\epsilon}{\zeta} \right) \zeta_{\tau\tau} = -2 + \epsilon \frac{3\zeta_\tau^2}{2\zeta^2} \qquad (\tau > 0), \tag{15}$$

$$\zeta(0) = 1, \quad \zeta_\tau(0) = 0, \tag{16}$$

where the non-dimensional parameter

$$\epsilon = \frac{\pi \rho_a R^4}{8 H_0 M} \tag{17}$$

is assumed to be much smaller than unity. In the case $\rho_a = 1\ \mathrm{kg\,m^{-3}}$, $R = 0{\cdot}1$ m, $H_0 = 0{\cdot}15$ m and $M = 2$ kg, we have $\epsilon = 0{\cdot}000131$. During the acceleration stage, when $\zeta(\tau) \gg \epsilon^{\frac{1}{2}}$ and $\epsilon \ll 1$, Equation (15) can be approximated as $\zeta_{\tau\tau} \approx -2$, which describes the motion of the falling disk in the absence of aerodynamic forces acting on it.

During the interaction stage, when $\zeta(\tau)$ is small, an asymptotic solution of Equation (15) as $\epsilon \to 0$ can be obtained. We introduce a new unknown function $w(\zeta) = \zeta_\tau^2$, the equation for which

$$\frac{\mathrm{d}w}{\mathrm{d}\zeta} = \frac{3\epsilon}{\zeta(\zeta+\epsilon)}w - \frac{4\zeta}{\zeta+\epsilon} \tag{18}$$

follows from (15). Conditions (16) yield

$$w(1) = 0. \tag{19}$$

The solution of the linear problem (18) and (19) provides

$$\frac{\mathrm{d}\zeta}{\mathrm{d}\tau} = -2\frac{\zeta^{\frac{3}{2}}(1-\epsilon^2-\zeta-2\epsilon\log\zeta+\epsilon^2/\zeta)^{\frac{1}{2}}}{(\zeta+\epsilon)^{\frac{3}{2}}}, \quad (\tau > 0) \tag{20}$$

$$\zeta(0) = 1.$$

Therefore, the solution of the original problem (15) and (16) is given by quadrature

$$\tau = \frac{1}{2}\int_\zeta^1 \frac{(v+\epsilon)^{\frac{3}{2}}\mathrm{d}v}{v\left[v(1-\epsilon^2)-v^2-2\epsilon v\log v+\epsilon^2\right]^{\frac{1}{2}}}. \tag{21}$$

The right-hand side of Equation (20) is never equal to zero for $0 < \zeta < 1$, which implies that the falling plate cannot change the direction of its motion. Formula (21) shows that the distance $H(t)$ between the plates decays as

$$H(t) \sim H_0 \exp\left(-2t/\left(T\epsilon^{\frac{1}{2}}\right)\right) \tag{22}$$

when $t \to \infty$. This result was obtained directly from Equations (1–7) by Yih [4]. Therefore, the velocity, at which the plates meet, is very small within the considered simplified model. However, the main events occur well before the asymptotic formula (22) becomes valid.

In order to describe the details of the plate interaction, we note that formula (22) is valid when $\zeta/\epsilon \ll 1$, which is the final stage of the interaction. When $\epsilon/\zeta \ll 1$, Equation (20) provides

$$\zeta(\tau) \approx 1 - \tau^2. \tag{23}$$

In dimensional variables the latter solution has the form $H(t) \approx H_0 - gt^2/2$ and corresponds to the plate motion at the acceleration stage. Therefore, the well-pronounced interaction between the plates occurs at the stage, when $\zeta(\tau) = O(\epsilon)$ as $\epsilon \to 0$.

We introduce the 'inner' variable $\sigma = \zeta/\epsilon$ and divide the integration interval in (21) into two parts $(\epsilon\sigma, \sqrt{\epsilon})$ and $(\sqrt{\epsilon}, 1)$. Both integrals are analyzed asymptotically as $\epsilon \to 0$ and $\sigma = O(1)$. Omitting details of the asymptotic analysis, we present the final result

$$\frac{1}{\epsilon}\left[\tau(\epsilon\sigma,\epsilon) - \tau_*(\epsilon)\right] = G(\sigma) + O\left(\sqrt{\epsilon}\log\epsilon\right), \tag{24}$$

$$G(\sigma) = \frac{2-\sigma}{2\sqrt{\sigma}}\sqrt{1+\sigma} - \frac{3}{2}\log\left(\sqrt{1+\sigma}+\sqrt{\sigma}\right), \tag{25}$$

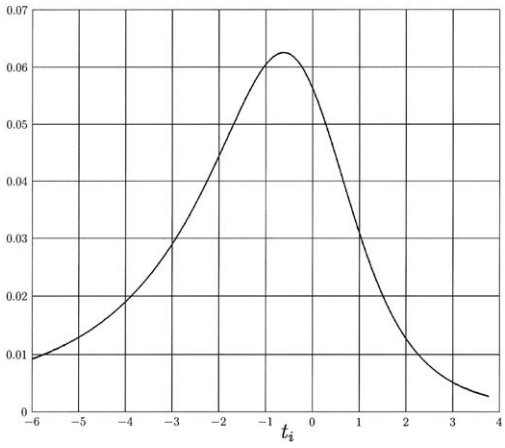

Figure 3. Non-dimensional aerodynamic force as function of the stretched time.

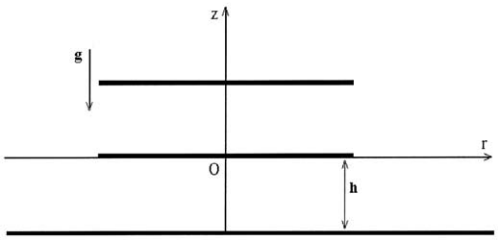

Figure 4. Acceleration of floating plate by another one falling on it.

$$\tau_*(\epsilon) = 1 - \frac{3}{4}\epsilon \log \epsilon + \epsilon \left(\log 2 - \frac{3}{4} \right).$$

The function $\tau_*(\epsilon)$ defines the time shift. The asymptotic solution (24) was justified with the help of direct numerical simulation of Equation (20) for ϵ of the order of $O(10^{-4})$. It was shown that the difference between these two solutions is negligibly small. We conclude that the well-pronounced interaction between the plates occurs for distances of the order of $O(\epsilon H_0)$ and the duration of this stage is of the order of $O(\epsilon T)$.

When $\zeta = \epsilon\sigma$, $\sigma = O(1)$ and $\epsilon \to 0$, formula (20) gives the velocity of the moving plate

$$\frac{\mathrm{d}H}{\mathrm{d}t} \approx -\sqrt{2gH_0} \left(\frac{\sigma}{\sigma + 1} \right)^{\frac{3}{2}} \tag{26}$$

and formula (15) gives the acceleration of this plate as

$$\frac{\mathrm{d}^2 H}{\mathrm{d}t^2} \approx \frac{3g}{\epsilon} \frac{\sigma^2}{(\sigma + 1)^4}. \tag{27}$$

It is seen that the plate acceleration at the interaction stage is positive and is much greater than the acceleration due to gravity. The falling plate acceleration takes its maximal value $3g/(16\epsilon)$ at $\sigma = 1$. The aerodynamic force $F_a(t)$ given by (12) is equal approximately to

$$F_a(t) \approx \frac{3}{\epsilon} Mg \frac{\sigma^2}{(\sigma + 1)^4} \tag{28}$$

during the interaction stage. The maximum of the aerodynamic force $3Mg/(16\epsilon)$ is much greater than the gravity force Mg. Figure 3 shows the non-dimensinonal quantity $\epsilon F_a(t)/(3Mg)$ as the function of the 'inner' stretched time $t_i = (\tau - \tau_*)/\epsilon$. In stretched variables the maximum of the function, 1/16, occurs at $t_i = G(1)$.

The pressure between the plates is maximal at the plate centre, where

$$p(0, t) \approx \frac{24Mg}{\pi\epsilon R^2} \frac{\sigma^2}{(\sigma + 1)^4} \tag{29}$$

to leading order as $\epsilon \to 0$. It is seen that the pressure cannot be higher than $(12M^2 g H_0)/(\pi^2 \rho_a R^6)$. The air can be treated as incompressible if the latter quantity is much smaller than the product $\rho_a c_a^2$, where c_a is the sound speed in the air, $c_a = 345$ m sec^{-1}. This condition yields

$$M^2 H_0 R^{-6} \ll \frac{\pi^2}{12g} \rho_a^2 c_a^2.$$

The right-band side of the inequality is equal approximately to 1686000 kg^2 m^{-5} for $\rho_a = 1{\cdot}29$ kg m^{-3} and $g = 9{\cdot}81$ m sec^{-2}, which implies that the air compressibility can be safely neglected for light falling plates. When ϵ is very small, the distance between the plates at the interaction stage is also small and the viscious effects have to be taken into account. This problem is not considered here. We conclude that the simple formulae (26–29) provide approximate description of the plate interaction if the falling plate is light.

3. Acceleration of circular plate

We consider here the same problem as that of Section 2 but now the lower plate is free to move (see Figure 1). The lower plate of mass m is initially at rest. Its weight is balanced by a weak elastic thread [1]. The motion of this plate is initiated by its interaction with another circular plate of the same radius R, which is falling down from a height H_0. We consider the interaction stage of the process, during which the lower disk is accelerated and its displacement $z_0(t)$ is so small that the restoring force due to the elastic thread can be neglected, Only the flow of the air between the plates is taken into account. The distance $H(t)$ between the plates is equal to $z_1(t) - z_0(t)$, where $H_0 - z_1(t)$ is the displacement of the falling plate, $z_0(0) = 0$, $\dot{z}_0(0) = 0$, $z_1(0) = H_0$ and $\dot{z}_1(0) = 0$.

In the same manner as it was done in Section 2 we obtain the velocity potential between the moving plates in the form

$$\phi(r, z, t) = -\frac{\dot{H}}{4H}\left[r^2 - 2(z - z_0(t))^2\right] + \dot{z}_0 z + \phi_0(t)$$

and the air pressure as

$$p(r, z, t) = \rho_a \left[r^2 \left(\frac{\ddot{H}}{4H} - \frac{3\dot{H}^2}{8H^2} \right) - (z - z_0(t))^2 \frac{\ddot{H}}{2H} - \ddot{z}_0 z - \frac{1}{2}\dot{z}_0^2 - \dot{\phi}_0(t) \right], \tag{30}$$

where $z_0(t) < z < z_1(t)$. The second, third and fourth terms in (30) can be neglected compared to the first one with a relative error of $O(H^2/R^2)$ during the interaction stage when $z - z_0(t) = O(H)$, $\dot{z}_0(t) = O(\dot{H})$, $\ddot{z}_0(t) = O(\ddot{H})$ and $H/R \ll 1$. The boundary condition $p(R, z, t) = 0$ and Equation (30) provide

$$\dot{\phi}(t) = R^2 \left(\frac{\ddot{H}}{4H} - \frac{3\dot{H}^2}{8H^2} \right) + O\left(\frac{H^2}{R^2} \right).$$

The obtained approximate formula for the pressure between the plates is identical to (11). We conclude that with a relative error up to $O(H^2/R^2)$, the pressure distribution between the moving circular plates depends on the distance between them but not on their relative motions. In particular, the aerodynamic force, $F_a(t)$ acting on the plates is given by Equation (12), where now $H(t) = z_1(t) - z_0(t)$.

Equations of the plate motion

$$M\frac{\mathrm{d}^2 z_1}{\mathrm{d}t^2} = -Mg + F_a(t), \tag{31}$$

$$m\frac{\mathrm{d}^2 z_0}{\mathrm{d}t^2} = -F_a(t), \tag{32}$$

where it has been taken into account that aerodynamic forces of same magnitude $F_a(t)$ act on both the upper and the lower plates and the weight of the lower plate is balanced by the elastic thread, and the equation for the distance between the plates $H(t)$ are as follows:

$$M\nu\frac{\mathrm{d}^2 H}{\mathrm{d}t^2} = -M\nu g + F_a(t), \qquad \nu = \frac{m}{m+M}. \tag{33}$$

Equation (33) is identical to Equation (6), where $F_a(t)$ is given by (12), derived for the case of a fixed lower plate. It is seen that, in the case of a free lower plate, the evolution of the distance $H(t)$ between the plates is the same as that in the problem of a fixed lower disk, but for which the mass of the falling plate is reduced by a factor ν. In particular, the asymptotic formulae (24–29) with the reduced mass of the falling plate are also valid for the present problem. Formula (26) shows that the relative difference between the velocities of the plates is less than 1% when $\sigma < \frac{1}{20}$. Therefore, we can conclude that the plates move together at the end of the interaction stage, when the distance between the plates is less than $\epsilon_m/20$, where ϵ_m is given by formula (17) with M substituted by $M\nu$. However, formula (26) says nothing about the final velocity v_f of the plate motion.

In the case of rigid impact, when the presence of air is not taken into account, the momentum conservation law yields

$$\sqrt{2gH_0}M = (M+m)v_f^R, \tag{34}$$

where v_f^R is the velocity of the plates after the impact and $\sqrt{2gH_0}$ is the velocity of the falling plate before the impact. Equation (34) introduces the quantity v_f^R. Substituting (12) in Equation (32) and integrating the latter one with respect to time, we obtain with the help of (20) and (34)

$$-\dot{z}_0(t) = v_f^R\left[\epsilon_m\frac{\sqrt{g(\zeta,\epsilon_m)}}{(\zeta+\epsilon_m)^{\frac{3}{2}}} + \frac{\epsilon_m}{2}\int_\zeta^1 \frac{\sqrt{g(u,\epsilon_m)}\mathrm{d}u}{u(u+\epsilon_m)^{\frac{3}{2}}},\right] \tag{35}$$

where $g(\zeta,\epsilon) = \epsilon^2 + \zeta(1-\epsilon^2-\zeta-2\epsilon\log\zeta)$ and $\zeta = H/H_0$. During the interaction stage, when $\zeta = \epsilon_m\sigma$ and $\sigma = O(1)$, formula (35) can be simplified to

$$-\dot{z}_0(t) = v_f^R\left[1 - \left(\frac{\sigma}{\sigma+1}\right)^{\frac{3}{2}} + O(\epsilon_m)\right],$$

when $\epsilon_m \to 0$. It is seen that the presence of air does not change the final velocity of the plate motion but makes the interaction smooth in contrast to the rigid-impact case.

Integrating Equation (32) twice with respect to time and taking into account the initial conditions and Equations (12), (20), (21) and (34), we find

$$z_0(t) = \frac{1}{2}\epsilon_m v_f^R T\left[\log\zeta - \frac{1}{2}\int_\zeta^1\left(\int_\zeta^\omega \frac{(v+\epsilon_m)^{\frac{2}{2}}\mathrm{d}v}{v\sqrt{g(v,\epsilon_m)}}\right)\frac{\sqrt{g(\omega,\epsilon_m)}\mathrm{d}\omega}{\omega(\omega+\epsilon_m)^{\frac{3}{2}}}\right],$$

where the double integral is of the order of $O(1)$ as $\epsilon_m/\zeta = O(1)$, *i.e.*, during both the acceleration and the interaction stages. Therefore, the displacement of the lower plate is given approximately as

$$z_0(t) = \frac{1}{2}\epsilon_m v_f^R T \log\zeta + O(\epsilon_m).$$

By the time the difference between the plate velocities drops down to 1%, we have $\zeta \approx \epsilon_m/20$ and

$$|z_0^*| = \frac{1}{2} v_f^R T \epsilon_m \log\frac{20}{\epsilon_m}.$$

When $M = 2$ kg, $m = 0{\cdot}22$ kg, $H_0 = 15$ cm and $R = 10$ cm, one gets $\epsilon_m \approx 0{\cdot}00132$, $v_f^R \approx 1{\cdot}55$ m sec^{-1}, $T = 0{\cdot}175$ sec and $|z_0^*| \approx 2$ mm. Therefore, the interaction stage lasts several milliseconds and the displacement of the lower plate at the end of this stage is estimated as 2 mm. The plates move as a whole at the velocity v_f^R at the end of the interaction stage. We can conclude that, from a kinematic point of view, the assumption of rigid type of plate collision (34) provides a good approximation of the plate velocity after impact. However, from a dynamic point of view, the presence of air leads to a finite acceleration of the lower plate and to finite forces between the plates during their interaction.

4. Impact onto floating circular disk

We consider the unsteady problem of acceleration of a floating circular disk of radius R by another disk of the same radius falling on it (see Figure 4). The initial stage of the flow, during which the hydrodynamic pressure in the liquid layer of thickness h takes its maximum value, is studied. The liquid layer is assumed to be thin, $h/R \ll 1$, allowing us to use the shallow-water approximation for the liquid flow beneath the plate. We assume that the duration of the initial stage is greater than the time scale R/c_0 of acoustic effects in the liquid. In the the case of water, $c_0 = 1500$ m sec^{-1}, and $R = 10$ cm, we have $R/c_0 \approx 7 \times 10^{-5}$ sec. The weight of the floating plate is balanced by a weak elastic thread which does not affect the plate displacement during the initial stage. The draft of the floating plate is zero. The initial stage, during which the floating plate is accelerated, is of short duration (see Section 3) and the displacement of the floating plate is small. That is why we can neglect the deformation of the liquid layer during this stage, linearize the boundary conditions and impose them on the initial position of the liquid boundary $z = 0$. Moreover, the equations of the liquid flow can also be linearized.

The liquid flow is described by the velocity potential $\varphi(r, z, t)$, which satisfies the following equiations

$$\frac{\partial^2\varphi}{\partial r^2} + \frac{1}{r}\frac{\partial\varphi}{\partial r} + \frac{\partial^2\varphi}{\partial z^2} = 0 \qquad (-h < z < 0, r > 0), \tag{36}$$

$$\frac{\partial\varphi}{\partial z} = \dot{z}_0(t) \qquad (z = 0, 0 < r < R), \tag{37}$$

$$\frac{\partial\varphi}{\partial z} = 0 \qquad (z = -h, r > 0), \tag{38}$$

$$\varphi = 0 \qquad (z = 0, r > R), \tag{39}$$

$$\varphi \to 0 \qquad (r \to \infty), \tag{40}$$

where $z_0(t)$ is the displacement of the floating disk. It is seen that

$$\varphi(r, z, t) = \dot{z}_0(t)\tilde{\varphi}(r, z) \tag{41}$$

with $\tilde{\varphi}(r, z)$ satisfying Equations (36), (38–40) and the boundary condition $\partial\tilde{\varphi}/\partial z = 1$ on the disk. During the initial stage the pressure distribution $p_\ell(r, z, t)$ in the liquid layer is given as

$$p_\ell(r, z, t) = -\rho\ddot{z}_0(t)\tilde{\varphi}(r, z). \tag{42}$$

Correspondingly, the hydrodynamic force $F_\ell(t)$ on the floating disk is defined by

$$F_\ell(t) = -2\pi\rho\ddot{z}_0(t)\int_0^R \tilde{\varphi}(r, 0)r\,\mathrm{d}r \tag{43}$$

within this approximation. Equation (43) can be rewritten as

$$F_\ell(t) = -\ddot{z}_0(t)M_a, \tag{44}$$

where M_a is the added mass of the floating disk.

The displacement $z_1(t)$ of the falling plate is described by Equation (31) with the aerodynamic force $F_a(t)$ given by (12) and $H(t) = z_1(t) - z_0(t)$ being the distance between the plates at time t. The motion of the floating plate is governed by the equation

$$m\frac{\mathrm{d}^2 z_0}{\mathrm{d}t^2} = -F_a(t) + F_\ell(t) \tag{45}$$

with the hydrodynamic force $F_\ell(t)$ given by (44). Hence, Equation (45) can be written in the form

$$(m + M_a)\frac{\mathrm{d}^2 z_0}{\mathrm{d}t^2} = -F_a(t), \tag{46}$$

which is identical with (32). The motion of the floating plate is described by the same equation as if the plate were free but of mass equal to $m + M_a$.

Equations (42) and (46) yield

$$p_\ell(r, z, t) = \frac{\rho F_a(t)}{m + M_a}\tilde{\varphi}(r, z). \tag{47}$$

The function $F_a(t)$ is given by (12), where $H = H_0\zeta(\tau)$ and $\zeta(\tau)$ is defined by Equations (15) and (16) with ϵ being now

$$\epsilon = \frac{\pi\rho_a R^4(m + M + M_a)}{8H_0 M(m + M_a)}. \tag{48}$$

The velocity potential $\tilde{\varphi}(r, z)$ was obtained by Vorovich and Yudovich [5] in the case of large thickness of the liquid layer, $h/R > \frac{2}{\pi}\log 2$, and by Chebakov [6] for a liquid layer of small thickness, $h/R < 1$. The second-order approximation of the potential $\tilde{\varphi}(r, z)$ as $h/R \to 0$ is derived below by means of an asymptotic method which can be helpful to treat more complicated shapes of a plate floating on a thin liquid layer.

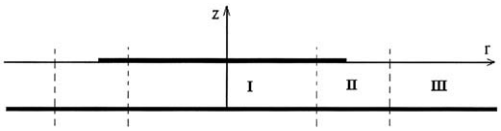

Figure 5. Decomposition of the thin region for asymptotic analysis of flow within it.

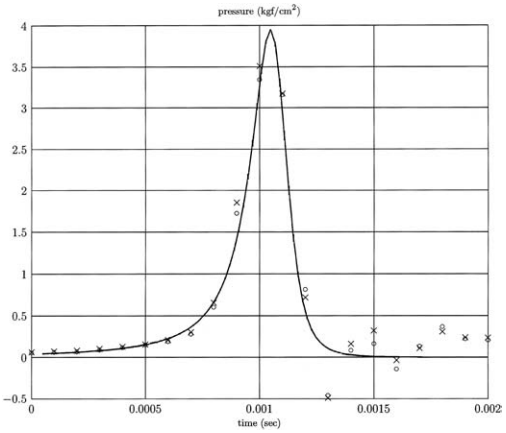

Figure 6. Pressure at the center of the floating plate in the case of the drop height of 15 cm and water depth of 2 cm [1 kgf cm^{-2} = 9 · 81 × 10^4 Nm^{-2}].

In order to construct the approximate solution of the boundary-value problem for the potential $\tilde{\varphi}(r, z)$, the method of matched asymptotic expansions is used. This method was used by Korobkin [7, 8] to study the hydraulic stage of the impact onto a shallow liquid layer. The flow region, $r > 0$, $-h < z < 0$, is divided into the following three parts shown in Figure 5: (I) the region beneath the floating plate; (II) the edge region and (III) the outer region.

In region I, the potential $\tilde{\varphi}(r, z)$ is sought in the form

$$\tilde{\varphi}(r, z) = \tilde{\varphi}_0(r) + \tilde{\varphi}_1(r)(z + h) + \frac{1}{2}\tilde{\varphi}_2(r)(z + h)^2 + \ldots, \tag{49}$$

where $r = O(R)$, $z = O(h)$ and $h/R \ll 1$. Substituting (49) in the Laplace equation (36) and in condition (38), we find

$$\tilde{\varphi}_1(r) \equiv 0, \qquad \tilde{\varphi}_2(r) = -\tilde{\varphi}_0^{''}(r) - r^{-1}\tilde{\varphi}_0^{'}(r). \tag{50}$$

A prime stands for the derivative with respect to the radial coordinate r. The condition $\partial\tilde{\varphi}/\partial z = 1$ on the floating plate for $z = 0$, $r < R$ and Equations (49) and (50) provide

$$\tilde{\varphi}_0^{''}(r) + r^{-1}\tilde{\varphi}_0^{'}(r) = -h^{-1}. \tag{51}$$

The solution of Equation (51) that is bounded in region I has the form

$$\tilde{\varphi}_0(r) = -\frac{r^2}{4h} + A. \tag{52}$$

Substituting (52) in (49) and taking (50) into account, one gets

$$\tilde{\varphi}(r, z) = -\frac{r^2}{4h} + A + \frac{1}{2h}(z + h)^2. \tag{53}$$

It is worth noticing that $\tilde{\varphi}_n(r) \equiv 0$ for $n \geq 3$. The constant A has to be determined from the matching condition between the solutions calculated in regions I and II. Equations (49) and (53) explain well the use of solution (9) in the air-flow problem. The potential of the flow

(53) in region I is not valid close to the region boundary, $r = R$, where the flow is essentially two-dimensional.

In region III, where $r = O(R)$, $z = O(h)$ and $(r - R)/h \gg 1$, the liquid remains at rest. It can be shown that $\tilde{\varphi}(r, z) = O(\exp[-\pi(r - R)/(2h)])$ in this region.

In region II, the flow is described by the stretched 'inner' variables $\xi = (r-R)/h$, $\eta = z/h$ and $\tilde{\varphi}(R + h\xi, h\eta) = h\hat{\varphi}(\xi, \eta, \delta)$, where $\delta = h/R$ is a small parameter. The 'inner' potential $\hat{\varphi}(\xi, \eta, \delta)$ satisfies the equations

$$\frac{\partial^2\hat{\varphi}}{\partial\xi^2} + \frac{\partial^2\hat{\varphi}}{\partial\eta^2} = -\frac{\delta}{1+\delta\xi}\frac{\partial\hat{\varphi}}{\partial\xi} \qquad (-1 < \eta < 0, -\infty < \xi < \infty), \tag{54}$$

$$\frac{\partial\hat{\varphi}}{\partial\eta} = 0 \qquad (\eta = -1), \tag{55}$$

$$\hat{\varphi} = 0 \qquad (\eta = 0, \xi > 0), \tag{56}$$

$$\frac{\partial\hat{\varphi}}{\partial\eta} = 1 \qquad (\eta = 0, \xi < 0), \tag{57}$$

$$\hat{\varphi} \to 0 \qquad (\xi \to +\infty), \tag{58}$$

$$\hat{\varphi} \sim \frac{1}{\delta^2}\left[\frac{\delta^2 A}{h} - \frac{1}{4}\right] - \frac{1}{2\delta}\xi + \frac{1}{2}(\eta+1)^2 - \frac{1}{4}\xi^2 \qquad (\xi \to \infty). \tag{59}$$

Condition (58) follows from the matching between the 'inner' solution in region II and the solution in region III. Correspondingly, condition (59) follows from the matching of the 'inner' solution in region II to the solution (53) in region I. The matching condition (59) shows that the constant A can be determined in the form

$$A = h\delta^{-2}(A_0 + \delta A_1 + \delta A_2 + \ldots) \tag{60}$$

and the potential $\hat{\varphi}(\xi, \eta, \delta)$ has to be sought as

$$\hat{\varphi}(\xi, \eta, \delta) = \delta^{-2}\hat{\varphi}_0(\xi, \eta) + \delta^{-1}\hat{\varphi}_1(\xi, \eta) + \hat{\varphi}_2(\xi, \eta) + \ldots. \tag{61}$$

Substituting (60) and (61) in Equations (55–59) and collecting the terms of the same order with respect to δ^n, $n = -2, -1, 0, \ldots$, we obtain at first order ($n = -2$):

$$A_0 = \frac{1}{4}, \qquad \hat{\varphi}_0(\xi, \eta) \equiv 0 \tag{62}$$

and at second order ($n = -1$):

$$\frac{\partial^2\hat{\varphi}_1}{\partial\xi^2} + \frac{\partial^2\hat{\varphi}_1}{\partial\eta^2} = 0 \qquad (-1 < \eta < 0),$$

$$\frac{\partial\hat{\varphi}_1}{\partial\eta} = 0 \qquad (\eta = -1, \text{and } \eta = 0, \xi < 0),$$

$$\hat{\varphi}_1 = 0 \qquad (\eta = 0, \xi > 0), \tag{63}$$

$$\hat{\varphi}_1 \to 0 \qquad (\xi \to +\infty),$$

$$\hat{\varphi}_1 \sim A_1 - \frac{1}{2}\xi \qquad (\xi \to -\infty).$$

The solution of the boundary-value problem (63) was given by Noble [9, Chapter III, pp. 135–136].

The function $\hat{\varphi}_1(r, z)$ is not reproduced here. The solution exists if and only if

$$A_1 = \frac{1}{\pi}\log 2. \tag{64}$$

Equations (53), (60), (62) and (64) define the second-order velocity potential in region I as

$$\hat{\varphi}(r, z) = \frac{1}{4h}(R^2 - r^2) + \frac{R}{\pi}\log 2 + O(h). \tag{65}$$

The added mass M_a is defined by Equations (43) and (44). Using the asymptotic formula (65) and taking into account that the contribution of the 'inner' solution (61) to the added mass is of the order $O(\rho h R^2)$ and can he neglected compared to the contribution of solution (53), which is of the order $O(\rho R^4/h)$, with a relative error of $O(\delta^2)$, we obtain

$$M_a = \frac{\pi\rho R^4}{8h}\left[1 + \frac{8\log 2}{\pi}\delta + O(\delta^2)\right]. \tag{66}$$

Equations (47) and (65) show that the hydrodynamic pressure $p_\ell(r, z, t)$ depends weakly on the vertical coordinate z and takes its maximal value at the plate center, where

$$p_\ell(0, 0, t) = \frac{\rho R^2 F_a(t)}{4h(m + M_a)}\left[1 + \frac{4\log 2}{\pi}\delta + O(\delta^2)\right]. \tag{67}$$

During the interaction stage the aerodynamic force $F_a(t)$ is given by (28), where now the mass of the falling body has to be substituted by $M(m + M_a)/(M + m + M_a)$ and ϵ is given by (48). Therefore

$$p_\ell(0, 0, t) \approx P_{sc}\frac{\sigma^2}{(1 + \sigma)^4}, \tag{68}$$

$$P_{sc} = \frac{6}{\pi}\frac{\rho}{\rho_a}\left(\frac{M}{M + m + M_a}\right)^2 \frac{(m + M_a)gH_0}{hR^2}\left(1 + \frac{4\log 2}{\pi}\frac{h}{R}\right). \tag{69}$$

Here $\sigma = H(t)/(\epsilon H_0)$ and $t = T(\tau_* + \epsilon G(\sigma))$, the function $G(\sigma)$ is given by Equation (25), The scale P_{sc} of the impulsive pressure is proportional to the maximum of the hydrodynamic pressure on the bottom of the liquid layer. Formulae (68) and (69) are simple enough to be used at the design stage. Equation (69) shows that the hydrodynamic pressure due to the impact is strongly dependent on the air density ρ_a. If the air is wet as in sea conditions, the pressures will be smaller than in laboratory conditions.

In the case of infinite depth of the liquid Equations (47) and (48) are also valid. For a circular floating plate $\tilde{\varphi}(r, 0) = \frac{2}{\pi}\sqrt{R^2 - r^2}$ and $M_a = \frac{4}{3}\rho R^3$. The pressure at the plate center is given by (68), where P_{sc} is now

$$P_{sc} = \frac{48}{\pi^2}\frac{\rho}{\rho_a}\left(\frac{M}{M + m + M_a}\right)^2 \frac{(m + M_a)gH_0}{R^3}.$$

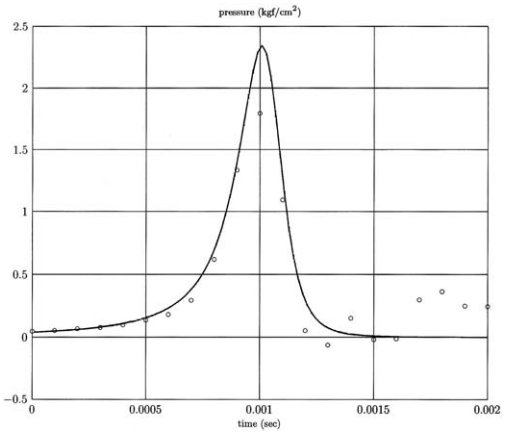

Figure 7. Pressure at the center of the floating plate in the case of the drop height of 15 cm and water depth of 4 cm [1 kgf cm^{-2} = 9 · 81 × 10^4 Nm^{-2}].

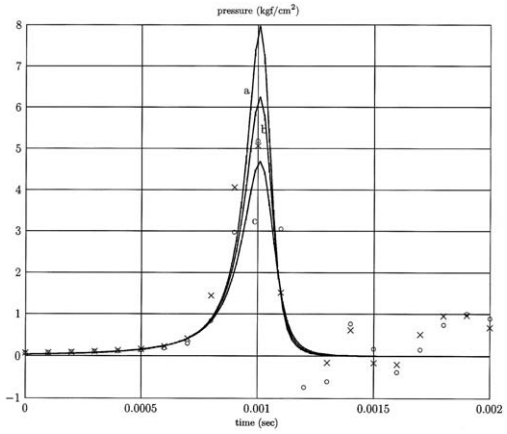

Figure 8. Pressure at the center of the floating plate in the cases of the drop heights of (a) 51 cm, (b) 40 cm, (c) 30 cm and water depth of 4 cm. Theoretical curves are shown with solid line [1 kgf cm^{-2} = 9 · 81 × 10^4 Nm^{-2}]. Experimental results by Ermanyuk [1] are for the drop height of 51 cm (crosses and circles).

Theoretical predictions based on Equations (24), (25) and (68), (69) are compared to the experimental results by Ermanyuk [1]. He measured the hydrodynamic pressure at the bottom of the liquid layer just beneath the center of the floating plate (see Figure 1). The experiments were performed under the following conditions: $M = 2$ kg, $m = 0{\cdot}22$ kg, $R = 10$ cm, $\rho = 1000\ \mathrm{kg\,m^{-3}}$, $\rho_a = 1{\cdot}29\ \mathrm{kg\,m^{-3}}$, drop heights $H_0 = 15$ cm and 51 cm, liquid depths $h = 2$ cm and $h = 4$ cm. For almost each combination of the drop height and the liquid depth the experiments were performed twice. In Figures 6, 7 and 8 the experimental results are shown by circles and crosses and the theoretical results by solid lines. Experimental results were recorded at the frequency of 10 KHz. It is seen that the simplified model presented in this paper overpredicts the pressure maximum but describes quite reasonably the variation of the pressure with time. The theoretical curves, in fact, are obtained by stretching Figure 3 in the horizontal direction by a factor $T\epsilon$ and in the vertical direction by a factor P_{sc} (see Equations (28) and (68)). In addition, theoretical curves for $H_0 = 40$ cm and $H_0 = 30$ cm are shown in Figure 8. It is seen that variations of the drop height change mainly the pressure magnitude but not so much the duration of the loads. This is because the time scale $T\epsilon$ of the stage under consideration is proportional to $H_0^{-\frac{1}{2}}$ and weakly depends on variations of H_0. The overestimation of the pressure magnitude in the developed theory may be due to the simplified description of the acceleration stage, when the distance $H(t)$ between the plates is large. During this stage the falling-plate motion is governed by the gravity force and by both the aerodynamic force and friction forces which are due to the presence of the guiding tube in the experiments. The latter two forces are neglected in the present analysis. They can be accounted for by reduction of the impact velocity $\sqrt{2gH_0}$ at the beginning of the interaction stage, which is by proper reduction of the drop height H_0. Figure 8 shows that this may be the case but other effects have also to be taken into account to provide a more accurate description of the pressure peak. Among these effects compressibility and viscosity of the air,

the resistance of the air outside the plates to the outflow from between the plates, elasticity of the plates and the compressibility of the liquid should be mentioned.

5. Conclusion

A simple model has been presented to account for the presence of air between two colliding circular plates. The obtained theoretical results describe well the evolution of the hydrodynamic pressure with time but overestimate its magnitude. Nevertheless, the theory can be used at the design stage and for planning new experiments on floating-body impact. It would be of importance to study this problem for bodies, the surfaces of which are not flat in the impact region but convex/concave.

It should be noted that the air-cushion effect can be reduced by using a perforated falling plate. In this case the collision will be rigid and high acoustic pressures in the liquid may be expected. However, the impact velocity of the falling plate due to its perforation and the corresponding dissipation of the body energy might be smaller than for a plate without holes.

The comparison of the theoretical results with the experimental ones shows that both the air compressibility and viscosity have to be taken into account, in order to improve the predictions.

Acknowledgements

A.A.K. gratefully acknowledges an appointment as Visiting Professor at the Kyushu University in the summer of 1998. The authors would like to thank Dr. E.V. Ermanyuk for fruitful discussions and providing the experimental results.

References

1. E.V. Ermanyuk, Report on the experimental study of body impact onto shallow water. *Internal report of RIAM* (1999) 19 pp.
2. E.V. Ermanyuk and M. Ohkusu, Impact of a disk on shallow water. *J. Fluids Struct.* (2003) (accepted).
3. A.A. Korobkin and D.H. Peregrine, The energy distribution resulting from an impact on a floating body. *J. Fluid Mech.* 417 (2001) 157–181.
4. C.-S. Yih, Fluid mechanics of colliding plates. *Phys. Fluids* 17 (1974) 1936–1940.
5. I.I. Vorovich and V.I. Yudovich, Circular disc impact on liquid of finite depth. *Prikl. Mat. Mech.* 21 (1957) 525–532.
6. M.I. Chebakov, Circular disc impact on liquid of small depth. *Prikl. Mat. Mech.* 38 (1957) 675–681.
7. A. Korobkin, Impact of two bodies one of which is covered by a thin layer of liquid. *J. Fluid. Mech.* 300 (1995) 43–58.
8. A. Korobkin, Shallow-water impact problems. *J. Engng. Math.* 35 (1999) 233–250.
9. B. Noble, *Methods Based on the Wiener-Hopf Technique.* London: Pergamon Press (1958) 246 pp.